Table 5 Logistic regression analysis of angiogenesis-related factors

Variable	Evaluation variable (cut-off point)	Odds ratio	95% CI	*P* value
VEGF	<47 × ≥47	0.480	0.095–2.426	0.375
t-PA	<2.3 × ≥2.3	2.250	0.574–8.824	0.245
VCAM-1	<2,370 × ≥2,370	16.000	1.735–147.541	0.014
ELAM-1	<70 × ≥70	0.716	0.187–2.744	0.626
IL-8	<10.0 × ≥10.0	3.250	0.761–13.889	0.112
PDGF	<1,450 × ≥1,450	3.666	0.907–14.813	0.068
Factor VIII	<181 × ≥181	0.545	0.140–2.120	0.382

The *t* test was used to compare baseline levels of angiogenesis-related parameters in terms of responders. A responder means a patient who showed CR, PR and SD; non-responders showed PD and NE

not associated with a worsening of liver function. The edema, associated with hypoalbuminemia, was managed with diuretics. The lack of hypertension as a toxic effect may have been due to the difference in the inhibitory profile between TSU-68, which strongly inhibits both PDGFR and VEGFR, and other antiangiogenic compounds, which predominantly inhibit VEGFR [21, 22].

From the viewpoint of the pharmacokinetics of TSU-68, no trend was seen toward higher plasma exposure to TSU-68 with greater liver dysfunction (Levels 1–3). Furthermore, the exposure in the patients with HCC appeared to be similar to that in patients with advanced solid tumors that were not HCC in a phase I study [15]. These findings suggest that impaired liver function is unlikely to affect the pharmacokinetics of TSU-68. The present study indicated that the C_{max} and AUC were reduced by the repeated administration of TSU-68, which has also been observed in previous trials [14, 15]. This decrease was found to be due to TSU-68, which caused an induction of its own metabolism in the non-clinical studies [12, 13]. Although in this study, the pharmacokinetics of TSU-68 was not examined after long-term consecutive oral administration, the AUC on day 28 has been reported to be similar to that on day 2. This suggests that the decreased exposure, which reaches steady state on day 2, is maintained throughout the therapeutic cycle. In Level 3, no obvious decrease in the AUC on day 2 was observed by reducing the dose of TSU-68 from 200 to 400 mg, although these results are based on a small amount of data. In addition, the estimated daily AUC in the patients who received 200 mg TSU-68 bid was roughly similar to the AUC data showing a 50% inhibition of human xenograft tumor growth in mice (data not shown). However, these data should be interpreted cautiously because the majority of the patients who were included as Child-Pugh B had Child-Pugh scores of 7.

In this study, we selected the fixed-dose for both Child–Pugh A and B because hepatitis or Child–Pugh A patients experienced toxicities (abdominal pain and diarrhea), although no DLT was found when 400 mg bid TSU-68 was

administered, and also because liver function may fluctuate between Child–Pugh A and B in the same patients. However, whether Child–Pugh A and B can be separated depends on the safety and PK profile of the drug. Patients with Child–Pugh A are initially recommended for clinical trials in HCC research [23], whereas the design of trials that include Child–Pugh B patients needs further investigation. In addition, whether Child-Pugh score is a good system for stratifying liver function with these types of drugs is open to argument.

Many agents targeting angiogenesis have been investigated in HCC [3, 4, 10, 11, 22, 24–27]. In an international phase III trial, sorafenib reduced the mortality hazard by 44% compared with placebo, with a median OS of 10.7 months (vs. 7.9 months with placebo) [3]. In an Asian phase III trial, patients who received sorafenib had a 35% disease control rate (vs. 16% with placebo), with a median TTP of 2.8 months (vs. 1.4 months) and a median OS of 6.5 months (vs. 4.2 months) [4]. The results mirrored those of the SHARP trial, although the Asia–Pacific patients had more advanced disease. In a phase I trial in Japan, sorafenib resulted in 4% PR and 83% SD, with a median TTP of 4.9 months and a median OS of 15.6 months [24]. Sunitinib, an inhibitor of VEGFR, PDGFR and c-Kit, was used against HCC in a phase II trial and produced a 3.9% PR and 38.5% SD, with a median progression-free survival of 3.9 months and a median OS of 9.8 months [22, 25]. Chemotherapy-naïve Child–Pugh A patients were enrolled in the sorafenib phase III trial [3, 4]. In our trial, eight Child–Pugh B patients were enrolled, and systemic chemotherapy had been already administered in 14 patients. The patients had been treated previously a mean of 8.2 times using various modalities. Although TTP in our trial is less than the reported data of SHARP [3] and similar to the Asian sorafenib trial in the placebo arms [4], these factors might affect the results.

The response rate (8.6%) and a median OS (13.1 months) of TSU-68 were comparable to those reported for these other agents. Some patients were

administered TSU-68 for more than 1 year after confirmed PD by independent review that was not determined by investigators, and the long-term treatment with TSU-68 might have contributed to the longer OS period. This warrants further study, but needs to be evaluated in a larger trial. Molecular-targeted agents, including TSU-68, generally show a relatively low response rate but a high disease control rate, indicating that a large proportion of patients reach SD. The treatment response assessed using RECIST may not accurately reflect the overall effect of these agents [23]. We had several cases in which necrosis was observed inside a tumor, despite the increase in tumor size. As an objective response is a weak surrogate of activity in phase II trials, a consensus conference endorsed by the American Association for the Study of Liver Diseases and the European Association for the Study of the Liver recommended the inclusion of TTP as the primary endpoint in phase II trials [23].

Molecular-targeted agents are being developed as systemic therapies for HCC in first- and second-line settings as monotherapy and in combination with locoregional therapies. The primary endpoint for phase III studies that assess primary HCC treatments is survival, and the control arm should be sorafenib. Comparison of single agents head to head with sorafenib might jeopardize study approval and the recruitment of patients for ethical reasons. For second-line treatments against advanced HCC, the new agents should be compared with placebo or best supportive care [23]. A phase II randomized study of TSU-68 in combination with TACE has been conducted (manuscript in preparation), and a phase III trial is being planned.

VEGF, PDGF and bFGF participate in the neovascularization of HCC [26, 27], and VEGF levels are thought to have a prognostic value [28]. IL-8 has proangiogenic activity in cancers, although its role in HCC is controversial [27]. Given that the primary target of TSU-68 is endothelial cells, we speculated that damaged vascular endothelial cells may release endothelial cell-specific markers such as sELAM-1 and sVCAM-1. As sVCAM-1 can be identified in the bloodstream, it is potentially useful as a non-invasive biomarker for the monitoring of disease progression in cancer [29]. A high level of VCAM-1 was significantly associated with an advanced disease stage and the presence of distant metastasis in gastric cancer [30] and also has been shown to be associated with angiogenesis and poor prognosis in breast cancer [31] and in HCC [32]. In this trial, we found higher baseline levels of sVCAM-1 in patients with good response (CR + PR + SD) after treatment with TSU-68. Although our data suggested that sVCAM-1 is a possible predictive marker for the response, the analysis is exploratory, and further study is necessary to confirm this possibility.

In conclusion, the step-wise study design based on hepatic function was useful in a safety assessment of TSU-68 in patients with HCC who had impaired liver function. The TSU-68 dosage of 200 mg bid has a favorable safety profile, even in patients with Child–Pugh B cirrhosis, and together with a high disease control rate, provides a rationale for its further evaluation in patients with HCC.

References

1. Parkin DM, Bray F, Ferlay J et al (2005) Global cancer statistics, 2002. CA Cancer J Clin 55:74–108
2. Bruix J, Sherman M (2005) Management of hepatocellular carcinoma. Hepatology 42:1208–1236
3. Llovet JM, Ricci S, Mazzaferro V et al (2008) Sorafenib in advanced hepatocellular carcinoma. N Engl J Med 359:378–390
4. Cheng AL, Kang YK, Chen Z et al (2009) Efficacy and safety of sorafenib in patients in the Asia-Pacific region with advanced hepatocellular carcinoma: a phase III randomised, double-blind, placebo-controlled trial. Lancet Oncol 10:25–34
5. Laird AD, Vajkoczy P, Shawver LK et al (2000) SU6668 is a potent antiangiogenic and antitumor agent that induces regression of established tumors. Cancer Res 60:4152–4160
6. Naumova E, Ubezio P, Garofalo A et al (2006) The vascular targeting property of paclitaxel is enhanced by SU6668, a receptor tyrosine kinase inhibitor, causing apoptosis of endothelial cells and inhibition of angiogenesis. Clin Cancer Res 12:1839–1849
7. Yorozuya K, Kubota T, Watanabe M et al (2005) TSU-68 (SU6668) inhibits local tumor growth and liver metastasis of human colon cancer xenografts via anti-angiogenesis. Oncol Rep 14:677–682
8. Solorzano CC, Jung YD, Bucana CD et al (2001) In vivo intracellular signaling as a marker of antiangiogenetic activity. Cancer Res 61:7048–7051
9. Kuenen BC, Giaccone G, Ruijter R et al (2005) Dose-finding study of the multitargeted tyrosine kinase inhibitor SU6668 in patients with advanced malignancies. Clin Cancer Res 11:6240–6246
10. Kanai F, Yoshida H, Teratani T et al (2006) New feasibility study design with hepatocellular carcinoma: a phase I/II study of TSU-68, an oral angiogenesis inhibitor [Abstract]. J Clin Oncol 24(Suppl):213S
11. Kanai F, Yoshida H, Tateishi R et al (2008) Final results of a phase I/II trial of the oral anti-angiogenesis inhibitor TSU-68 in patients with advanced hepatocellular carcinoma [Abstract]. J Clin Oncol 26(Suppl):235S
12. Kitamura R, Yamamoto Y, Nagayama S et al (2007) Decrease in plasma concentrations of antiangiogenic agent TSU-68 ((Z)-5-[(1, 2-dihydro-2-oxo-3H-indol-3-ylidene)methyl]-2, 4-dimethyl-1H-pyrrole-3-propanoic acid) during oral administration twice a day to rats. Drug Metab Dispos 35:1611–1616

Springer

13. Kitamura R, Asanoma H, Nagayama S et al (2008) Identification of human liver cytochrome P450 isoforms involved in autoinduced metabolism of the antiangiogenic agent (Z)-5-[(1, 2-dihydro-2-oxo-3H-indol-3-ylidene)methyl]-2, 4-dimethyl-1H-pyrrole-3-propanoic acid (TSU-68). Drug Metab Dispos 36:1003–1009
14. Ueda Y, Shimoyama T, Murakami H et al (2010) Phase I and pharmacokinetic study of TSU-68, a novel multiple receptor tyrosine kinase inhibitor, by twice daily oral administration between meals with solid tumors (under submission)
15. Murakami H, Ueda Y, Shimoyama T et al. (2010) Phase I, pharmacokinetic, and biological studies of TSU-68, a novel multiple tyrosine kinase inhibitor, administered after meals with solid tumors (under submission)
16. Green H, Benedetti J, Crowley J (2002) Clinical trials in oncology, 2nd edn. Chapman & Hall, London
17. Fleming TR (1982) One-sample multiple testing procedures for phase II clinical trials. Biometrics 38:143–151
18. The Liver Cancer Study Group of Japan (2000) The general rules for the clinical and pathological study of primary liver cancer. Version 4. Kanehara & Co., Ltd., Tokyo
19. Makuuchi M, Belghiti J, Belli G et al (2003) IHPA concordant classification of primary liver cancer: working group report. J Hepatobiliary Pancreat Surg 10:26–30
20. Llovet JM, Bruix J (2008) Novel advancements in the management of hepatocellular carcinoma 2008. J Hepatol 48:S20–S37
21. Roodhart JM, Langenberg MH, Witteveen E et al (2008) The molecular basis of class side effects due to treatment with inhibitors of VEGF/VEGFR pathway. Curr Clin Pharmacol 3:132–143
22. Faivre S, Raymond E, Boucher E et al (2009) Safety and efficacy of sunitinib in patients with advanced hepatocellular carcinoma: an open-label, multicentre, phase II study. Lancet Oncol 10:794–800
23. Llovet JM, Di Bisceglie AM, Bruix J et al (2008) Panel of experts in HCC-design clinical trials. Design and endpoints of clinical trials in hepatocellular carcinoma. J Natl Cancer Inst 100:698–711
24. Furuse J, Ishii H, Nakachi K et al (2008) Phase I study of sorafenib in Japanese patients with hepatocellular carcinoma. Cancer Sci 99:159–165
25. Zhu AX, Sahani DV, Duda DG et al (2009) Efficacy, safety, and potential biomarkers of sunitinib monotherapy in advanced hepatocellular carcinoma: a phase II study. J Clin Oncol 27:3027–3035
26. Thomas MB, Abbruzzese JL (2005) Opportunities for targeted therapies in hepatocellular carcinoma. J Clin Oncol 23:8093–8108
27. Pang R, Poon RT (2006) Angiogenesis and antiangiogenic therapy in hepatocellular carcinoma. Cancer Lett 242:151–167
28. Poon RT, Lau C, Pang R et al (2007) High serum vascular endothelial growth factor levels predict poor prognosis after radiofrequency ablation of hepatocellular carcinoma: importance of tumor biomarker in ablative therapies. Ann Surg Oncol 14:1835–1845
29. Alexiou D, Karayiannakis AJ, Syrigos KN et al (2001) Serum levels of E-selectin, ICAM-1, and VCAM-1 in colorectal cancer patients: correlations with clinicopathological features, patient survival and tumor surgery. Eur J Cancer 37:2392–2397
30. Alexiou D, Karayiannakis AJ, Syrigos KN et al (2003) Clinical significance of serum levels of E-selectin, intracellular adhesion molecule-1, and vascular cell adhesion molecule-1 in gastric cancer patients. Am J Gastroenterol 98:478–485
31. O'Hanlon DM, Fitzsimons H, Lynch J et al (2002) Soluble adhesion molecule (E-selectin, ICAM-1 and VCAM-1) in breast carcinoma. Eur J Cancer 38:2252–2257
32. Joanna WH, Ronnie TP, Cindy ST et al (2004) Clinical significance of serum vascular cell adhesion molecule-1 levels in patients with hepatocellular carcinoma. World J Gastroenterol 10:2014–2018

Hemorrhagic Complications of Percutaneous Radiofrequency Ablation for Liver Tumors

Eriko Goto, MD, Ryosuke Tateishi, MD, Shuichiro Shiina, MD, Ryota Masuzaki, MD,
Kenichiro Enooku, MD, Takahisa Sato, MD, Takamasa Ohki, MD, Yuji Kondo, MD,
Tadashi Goto, MD, Haruhiko Yoshida, MD, and Masao Omata, MD

Background: Although radiofrequency ablation (RFA) is widely accepted as a percutaneous treatment for liver tumors; serious complications may occur resulting in 0.1% to 0.5% mortality. This study analyzed the risk factors and management of hemorrhagic complications, such as hemoperitoneum, hemothorax, and hemobilia.

Methods: We performed 4133 RFA treatments in 2154 patients with primary and metastatic liver tumors from February 1999 to December 2007. Of these, we enrolled patients with hemorrhagic complications and reviewed their medical records thoroughly. The risk factors for each hemorrhagic complication were analyzed using unconditional logistic regression.

Results: Hemorrhagic complications occurred in 63 out of 4133 treatments (1.5%), including hemoperitoneum in 29 (0.7%), hemothorax in 14 (0.3%), and hemobilia in 20 (0.5%). Eleven, 8, and 4 of these patients, respectively, were categorized as major complications requiring blood transfusion or drainage. Two patients died after hemoperitoneum. Logistic regression analysis revealed large tumor size [odds ratio (OR) 1.06 per 1 mm increase in diameter] and low platelet count (OR 0.88 per 10,000/μL increase) were significant risk factors for hemoperitoneum. The location of tumor nodules was a significant risk factor for hemothorax (segment 7, OR 2.31) and hemobilia (segment 1, OR 3.30). Other factors, including the number of needle insertions or the duration of ablation, were not significant.

Conclusions: Although hemorrhagic complications were relatively rare with percutaneous RFA, specific treatments, such as blood transfusion and drainage, were required in some cases. Care must be taken, especially in high-risk patients.

Key Words: hepatocellular carcinoma, metastatic liver tumor, radiofrequency ablation, complication

Radiofrequency ablation (RFA) is now widely accepted as a minimally invasive treatment alternative to surgical resection for liver neoplasms.[1–6] Although the safety of RFA has been confirmed in general, various complications have been reported and large-scale multicenter surveys

showed mortality of up to 1.4%.[5,7–15] Among the major complications of RFA, hemorrhagic complications such as hemoperitoneum, hemothorax, and hemobilia are important because if left untreated, they may prove fatal.[9,16,17] At least some of these complications are specific to certain tumor conditions. For example, hemothorax is mainly caused by an injury to the intercostal arteries and so the risk of hemothorax accompanies the treatment of tumors at specific locations. The elucidation of risk factors for hemorrhagic complications is crucial for their prevention, early detection, and subsequent proper management. However, as the incidence of hemorrhagic complications is low, reported to be < 1%, [5,7–14,18,19] a fairly large total number of treatments would be required for appropriate analysis of these risk factors. In addition, multicenter settings may not be preferable for the analysis because the precise evaluation of the clinical course in each case of complication may require a thorough perusal of medical records.

Since the introduction of RFA in 1999, we have performed more than 4000 percutaneous RFA treatments for liver tumors, which probably constitute the largest single-center experience worldwide. Previously, we reported the incidence of major complications of RFA, including hemorrhagic complications, when the number of treatments reached 1000. We reported 4 cases (0.4% per treatment) of hemoperitoneum requiring blood transfusion, 1 case (0.1% per treatment) of hemothorax requiring thoracic drainage, and 3 cases (0.3% per treatment) of self-limiting hemobilia. However, the risk factors for these complications were not analyzed in the previous report because of the limited number of events. The total number of treatments has increased substantially since that time, and we believe that it is now possible to analyze the risk factors for hemorrhagic complications of RFA reliably. The management strategies of such complications also deserve to be documented. Therefore, we conducted this study to elucidate the clinical characteristics of hemorrhagic complications and to provide a proper path for their management.

PATIENTS AND METHODS

Patients

We studied consecutive 4133 cases with liver tumors treated with percutaneous RFA at the Department of Gastroenterology, University of Tokyo Hospital from February 1999 to December 2007. The inclusion criteria for RFA were: total bilirubin concentration < 3 mg/dL, platelet count $\geq 50 \times 10^3$/mm^3, and prothrombin activity $\geq 50\%$. Ascites was controlled beforehand by

using diuretics. Patients with portal vein tumor invasion or extrahepatic metastasis were excluded. We also excluded patients with a history of bilioenteric anastomosis or sphincterotomy, who are considered to be at high risk for hepatic abscess formation. In general, we performed RFA on patients with 3 or fewer lesions, all of which were 3 cm or smaller in diameter. However, we also performed ablation on patients who did not meet these conditions, if the procedure was thought likely to be clinically effective.[20] Similar indication criteria were applied to metastatic liver tumors with controlled extrahepatic lesions.

The clinical data on each patient who underwent RFA in the authors' department were stored in a database designed and maintained prospectively to assess the short-term and long-term efficacy and safety of RFA treatment. When a complication was observed, the type, severity, and clinical outcome were input to the database immediately according to the criteria described below. Written informed consent was obtained from each patient before RFA.

Technical Terms Describing RFA

We defined an RFA session as a single intervention episode that consisted of one or more ablations performed on one or more intrahepatic tumors. An RFA treatment was defined as the total effort to ablate one or more tumors consisting of one or more sessions according to the working party report on image-guided tumor ablation.[21]

Diagnosis of Liver Tumors

Hepatocellular carcinoma (HCC) was diagnosed on the basis of typical findings on contrast-enhanced computed tomography (CT) or magnetic resonance imaging: hyper-attenuation in the arterial phase and hypoattenuation in the portal-venous phase.[22] When the imaging diagnosis was not conclusive, the diagnosis of HCC was confirmed histopathologically using an ultrasound-guided biopsy, based on the criteria of Edmondson and Steiner.[23] Metastatic liver tumors were diagnosed with enhanced CT or magnetic resonance imaging based on an increase in the size or number of lesions or changes in the enhancement pattern, through the course of disease. An ultrasound-guided biopsy was performed when necessary. A primary malignancy was histologically proven in each patient with a metastatic liver tumor.

RFA Procedures

The procedure of RFA has been described meticulously elsewhere.[5] In brief, ultrasound-guided percutaneous RFA was performed under local anesthesia, using a 17-gauge cooled-tip electrode (Cool-tip; Covidien, Mansfield, MA) with a 2 cm or 3 cm exposed tip. Multiple ablations were performed when the target nodule exceeded 2 cm in diameter. When the total ablation time for one treatment exceeded 60 minutes, we divided the treatment into 2 or more sessions to reduce the burden on the patient. When tumor ablation appeared to be completed, dynamic CT was performed 1 to 3 days after the last session with a slice thickness of 5 mm to evaluate treatment efficacy. On the basis of the CT findings, complete ablation was defined as nonenhancement in the entire lesion(s) with a safety margin in the surrounding liver parenchyma. When complete ablation was not attained, patients underwent additional sessions of ablation until complete ablation was confirmed in each nodule.

Monitoring After RFA Treatment

RFA was performed exclusively on an inpatient basis. At the end of the RFA session, the patients were screened with ultrasonography for echo-free space on the surface of the liver or in Morrison pouch caused by intraperitoneal bleeding and for biliary bleeding. After each RFA session, the patients were observed intensively with vital sign monitoring every 4 hours and checked for symptoms, such as strong pain not controlled with ordinary analgesics. Patients were strictly confined to bed overnight, first with complete rest and then rolling over was permitted 4 hours after ablation. Bed rest was relaxed after suitable blood test results were confirmed the next morning. When there was hypotension (systolic pressure < 90 mm Hg), tachycardia (heart rate > 100 beat/min), unusual pain, or other signs or symptoms of hemorrhage, we immediately checked the blood cell count and performed abdominal ultrasonography while monitoring with electrocardiogram and sphygmomanometer. A decrease in hemoglobin concentration by more than 10% of baseline was thought to suggest hemorrhage and the patient was monitored vigilantly at least every 4 hours. Fluid replacement commenced and blood transfusion was considered when the hemodynamics could not be stabilized.

Definition of Bleeding Complications With RFA

We adopted the described terminology concerning complications related to RFA.[24] In this study, we focused on the analysis of hemorrhagic complications, such as hemoperitoneum, hemothorax, and hemobilia. Hemoperitoneum was diagnosed when an echo-free space was detected with abdominal ultrasonography on the surface of liver or in Morrison pouch. Hemothorax was diagnosed when an echo-free space was found in the thorax or high-density fluid was found in the thorax on CT, which was performed routinely 1 to 3 days after RFA to evaluate treatment efficacy. Hemobilia was diagnosed when high-echogenic fluid appeared in the gallbladder (hemobilia sign) or high-density fluid was detected in the gallbladder on routine follow-up CT. Sometimes, hemobilia was confirmed on emergency upper gastrointestinal endoscopy indicated by hematemesis.

Chart Review

We searched the database and identified patients who had hemorrhagic complications and then we reviewed their medical records thoroughly. The following details were investigated meticulously: (1) the initial signs or symptoms, (2) the interval between RFA and the diagnosis of a complication, (3) the sequential changes in the hemoglobin concentration, and (4) the necessity of blood transfusion or other therapeutic procedures, such as thoracic or biliary drainage.

Risk Assessment

The incidence of hemorrhagic complications was assessed on a treatment basis (ie, the number of events divided by the total number of RFA treatments), because each treatment can be considered as an independent event with distinct tumor and host characteristics. The variables assessed in the analysis of risk factors for hemorrhagic complications were as follows: age, sex, HCC versus metastatic liver tumor, maximum tumor diameter, number of nodules, location of each nodule as classified using Couinaud liver segments,[25] number of RFA sessions, total

number of needle insertions, total duration of ablation, and laboratory data obtained immediately before RFA, including the platelet count and prothrombin activity. For each type of hemorrhagic complication, each variable was compared between the patients with and without that complication, using the Student t test for continuous variables and the χ^2 test or Fisher exact test for nominal variables. Unconditional multivariate logistic regression analysis was performed to assess the risk factors for each hemorrhagic complication. Differences with $P < 0.05$ were considered statistically significant. All statistical analyses were performed with S-PLUS 2000 (Insightful, Seattle, WA).

RESULTS

Patients

During the study period, 1864 patients underwent RFA for HCC. As 1022 of the patients received RFA 2 times or more for recurrent lesions at some interval (eg, 2 y), the total number of treatments was 3802. In addition, 331 patients received RFA one or more times for other types of cancer, including metastatic liver tumors (290 patients), colorectal cancer (225 patients), breast cancer (28 patients), stomach cancer (27 patients), and pancreatic cancer and gastrointestinal stromal tumors (5 patients each). The total number of RFA treatments was 4133, consisting of 6921 sessions on 8417 nodules. The baseline characteristics of the patients are shown in Table 1, summarized by treatment. Two-thirds were male, and the

TABLE 1. Baseline Characteristics—Treatment Basis (n = 4133)

Factors	
Male, n (%)	2775 (67.1)
Age (y)*	68.7 ± 8.5 (31-91)
Platelet count (10^3/mm^3)*	125 ± 33 (50-669)
Prothrombin activity (international normalized ratio)*	0.82 ± 0.098 (0.539-1.009)
Albumin (g/dL)*	3.6 ± 0.5 (2.1-5.0)
Total bilirubin (mg/dL)*	1.0 ± 0.5 (0.2-2.9)
Diagnosis, n (%)	
Hepatocellular carcinoma	3802 (92.0)
Metastatic liver tumor	331 (8.0)
Number of nodules, n*	2.1 ± 1.6 (1-20)
Diameter of maximum nodule (cm)*	2.3 ± 1.1 (0.5-13.5)
Tumor location, n (%)	
S1	239 (2.8)
S2	648 (7.8)
S3	842 (10.0)
S4	998 (11.9)
S5	930 (11.0)
S6	1097 (13.0)
S7	1179 (14.0)
S8	2484 (29.5)
Number of sessions per treatment.*	1.7 ± 0.9 (1-9)
Number of electrode insertions per treatment, n*	3.8 ± 3.4 (1-42)
Duration of ablation per treatment (min)*	32.8 ± 33.1 (6-505)

Values are summarized on a treatment basis.
*Expressed as the mean ± SD (range).

mean age was 69 years. Targeted liver tumors were HCC in 92% of the cases. Tumor locations, classified into segments S1 to S8 according to Couinaud segments, are also shown in Table 1. S8 was the most frequent location of both HCC and metastatic tumors, whereas S1 was the least frequent location.

Hemoperitoneum

Hemoperitoneum occurred in 29 treatments (0.7%) and blood transfusions (ranging from 2 to 6 units) were required in 10 of those cases (Table 2). Abdominal pain increasing in intensity several hours after RFA was the most common symptom among the patients with hemoperitoneum. In particular, all 10 patients who required blood transfusions complained of severe abdominal pain necessitating analgesic administration. Severe hypotension (ie, a systolic blood pressure < 90 mm Hg) was seen in 7 patients (24.1%), of which 4 had shock liver with an increase in serum aspartate aminotransferase over 500 IU/L. No specific signs or symptoms were noted in 8 patients and none of these patients required blood transfusions.

Hemoperitoneum was suspected by a decrease in hemoglobin concentration routinely measured the next morning and confirmed by intra-abdominal echo-free space on ultrasonography. A typical case of hemoperitoneum is presented in Figure 1. A 72-year-old man developed systolic hypotension 4 hours after RFA and an echo-free space was found on abdominal ultrasonography. After 4 units of red cells were transfused, his general condition stabilized and he was discharged on day 9 after RFA. In total, 2 patients died after hemoperitoneum. One of them was transfused 4 units of red cell concentrate and 30 units of platelets for hemoperitoneum. Although the intraperitoneal hemorrhage stopped without further intervention, this patient had a history of pulmonary lobectomy and developed acute respiratory distress syndrome on day 3 before eventually dying on day 15 after RFA. The other patient had a hepatic venous infarction with RFA and developed hemoperitoneum on day 5 after RFA. This patient died of liver failure on day 54. The delayed hemorrhage was exceptional and the hemoperitoneum was detected within 24 hours after RFA in all of the other patients.

Hemothorax

Hemothorax occurred in 14 treatments (0.3%). Three patients required both blood transfusion and thoracic drainage, whereas 2 other patients received blood transfusions only. All of the other patients recovered with conservative treatments only. Common symptoms were chest pain and dyspnea. However, about half of the cases of hemothorax were asymptomatic and detected during a routine CT taken to evaluate the efficacy of RFA. The 3 patients who required blood transfusions and thoracic drainage complained of right chest pain within 4 hours after RFA. The other 2 patients who received blood transfusion developed acute respiratory distress syndrome on days 4 to 6 after RFA, which was diagnosed as hypolucency in the right lung on chest x-ray and ground-glass appearance on chest CT. These patients were treated intensively with steroids and recovered. A case of hemothorax is shown in Figure 2. A 55-year-old man complained of right-sided chest pain immediately after RFA. The pain did not abate and hemothorax was diagnosed by the presence of an echo-free space in the right thorax on ultrasonography. He recovered and was discharged on day 20 after RFA.

— 81 —

TABLE 2. Symptoms of Each Complication at Diagnosis

	Hemoperitoneum (n = 29)	Hemothorax (n = 14)	Hemobilia (n = 20)
Hemoglobin decrease (g/dL)*	2.3 (0.5-4.5)	2.0 (1-3.6)	1.1 (0.1-3.2)
Patients with decrease in blood pressure, n (%)	7 (24.1)	1 (7.1)	1 (5.0)
Patients required blood transfusion, n (%)	10 (34.5)	3 (21.4)	1 (5.0)
Patients required drainage, n (%)	0	3 (21.4)	3 (15.0)
Interval from the procedure (h)*	17.9 (0-120)	13.7 (0-36)	4.8 (0-24)
Clinical symptoms, n (%)			
Abdominal pain	14 (48.3)	0	5 (25)
Chest pain	0	6 (42.9)	0
Dyspnea	0	2 (14.3)	0
Hematemesis	0	0	2 (10)

*Expressed as mean (range).

Hemobilia

Hemobilia was detected in 20 treatments (0.5%). Endoscopic biliary drainage was required in 3 cases. The appearance of high echogenicity in the gallbladder, designated as "hemobilia sign,"[26] during the RFA procedure led to the diagnosis of hemobilia in 8 cases, including 3 cases that were subsequently treated with biliary drainage. Blood transfusion was required in 1 case as the hemoglobin concentration decreased from 8.8 to 7.0 g/dL. The other decreases in the hemoglobin concentration with hemobilia were usually mild compared with hemoperitoneum or hemothorax and hypovolemic shock was not noted in any case. Symptoms related to hemobilia included upper abdominal pain, either right sided or median, and hematemesis. However, the severity of hemobilia did not depend on the severity of symptoms or decrease in hemoglobin concentration, but on the occurrence of biliary obstruction due to a blood clot. Biliary drainage was indicated when the total bilirubin concentration exceeded 4 mg/dL and the ultrasonographic findings indicated biliary obstruction. The interval between RFA and biliary drainage was 4 to 12 days and the average serum bilirubin concentration during drainage was 7.3 mg/dL (range: 4.8 to

FIGURE 1. A case of hemoperitoneum. Hemoperitoneum was diagnosed based on an intra-abdominal echo-free space on ultrasonography.

8.6). One case of hemobilia, a 78-year-old woman, is shown in Figure 3. The presence of hemobilia and a postprocedural increase in the bilirubin concentration suggested hemobilia-related biliary obstruction. Blood clots were removed endoscopically from the common bile duct on day 8. She recovered rapidly and was discharged on day 17.

Risk Factors

We analyzed the risk factors for each hemorrhagic complication (Table 3). Large tumor size [odds ratio (OR) 1.06 per 1 mm increase in diameter] and low platelet count (OR 0.88 per $10^3/mm^3$ increase) were significant risk factors for hemoperitoneum. The location of the tumor nodule was a significant risk factor for hemothorax (segment 7, OR = 2.31) and hemobilia (segment 1, OR = 3.30). Other factors, including the number of needle insertions and duration of ablation, were not found to be significantly associated with hemorrhagic complications.

DISCUSSION

The management of complications of invasive procedures can be classified into 2 categories: (1) the risk assessment before and during the procedure and (2) the prompt detection and treatment in cases with complications. General measures to prevent complications in RFA include the use of high-quality imaging devices, the assessment of bleeding tendency, availability of platelets or fresh frozen plasma transfusion when indicated, and the careful selection of the needle insertion route and body position during the procedure. The aim of postprocedural management is to detect complications and commence appropriate treatments promptly to avoid serious after effects.

Hemoperitoneum is presumably caused by an injury to the vasculature along the route of needle insertion. However, we noticed no puncturing of large intrahepatic vessels in cases of hemoperitoneum and suspect that injuries to small vessels not visible on ultrasonography are usually the origin of hemorrhage. Once bleeding begins, the possibility of hemostasis depends on platelet function and coagulation activity. Indeed, thrombocytopenia was found to be a significant risk factor for hemoperitoneum in this study. Although we set a minimum platelet count of $50 \times 10^3/mm^3$ as an inclusion criterion for RFA, preprocedural platelet transfusion may be considered if the platelet count is in the lower range. The location of the tumor, such as the proximity to the liver surface, was not associated with an
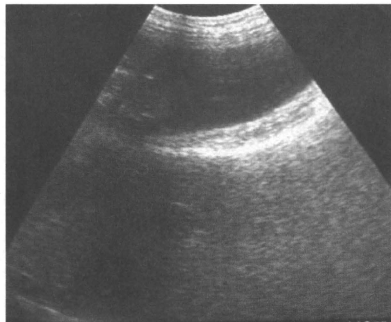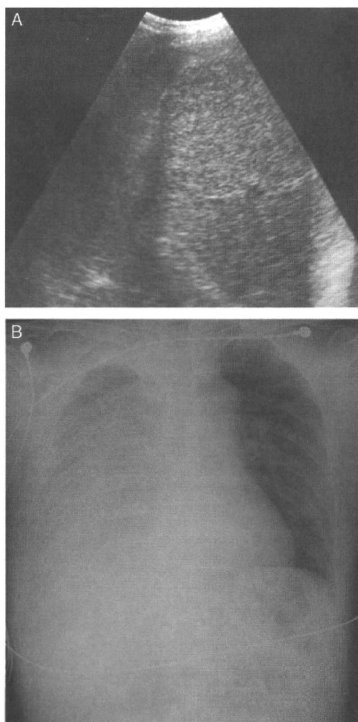
FIGURE 2. A case of hemothorax. A, A 55-year-old man with hemothorax after radiofrequency ablation, diagnosed based on an echo-free space in the right thorax on ultrasonography. B, Chest x-ray. Fluid was compressing the thorax, resulting atelectasis in the right lung.

increased risk of hemoperitoneum. The size of the tumor was found to be a risk factor, particularly when increased arterial blood flow may be involved. The usefulness of needle tract ablation to prevent hemoperitoneum, although not performed by our group, needs future evaluation.

Once intraperitoneal bleeding has occurred, it is important to prevent hypovolemic shock, shock liver, and subsequent liver failure. In our series, tachycardia (> 100 beat/min) was rarely observed before the systolic blood pressure fell below 100 mm Hg. Cirrhotic patients are often already in a hyperdynamic circulatory state and the appearance of tachycardia may delay hypovolemia. In the postprocedural management of HCC patients with cirrhosis, even mild tachycardia should excite attention.

Hemothorax, usually caused by puncturing an intercostal artery, is an arterial hemorrhage, and the platelet count is less strongly associated with hemothorax than with
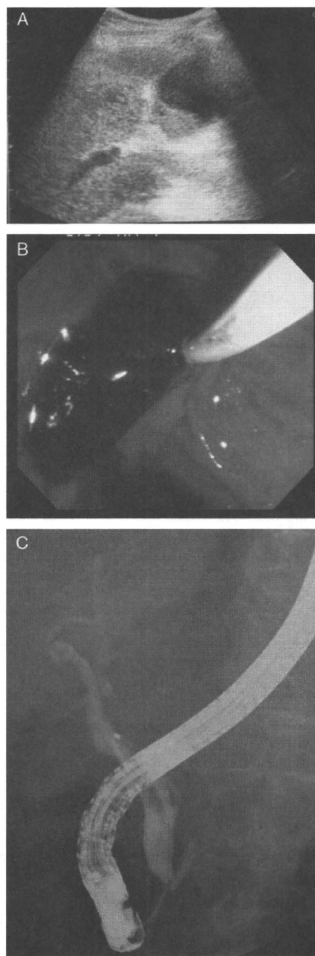
FIGURE 3. A case of hemobilia. A, A 78-year-old woman with hepatocellular carcinoma showed a high echoic area in the gallbladder. B, Hemobilia was confirmed on upper gastrointestinal endoscopy as bleeding from the papilla of Vater. C, The blood clots were removed from the common bile duct endoscopically.

hemoperitoneum. The risk of hemothorax is dependent on the route of insertion, and the ablation of tumors in the right lobe usually requires an intercostal approach. In

TABLE 3. Risk Factors for Bleeding Complications

Variables	Hemoperitoneum		Hemothorax		Hemobilia	
	OR (95% CI)	P	OR (95% CI)	P	OR (95% CI)	P
Male sex	0.869 (0.40-1.88)	0.722	1.730 (0.460-6.45)	0.418	0.806 (1.20-9.09)	0.658
Age (per 1 y)	1.008 (0.96-1.05)	0.727	1.001 (0.935-1.07)	0.970	1.003 (0.950-1.06)	0.919
Size (per 1 cm)	1.055 (1.021-1.09)	0.0014	0.995 (0.931-1.06)	0.871	1.037 (0.993-1.08)	0.104
Platelet count (per $10 \times 10^3/mm^3$)	0.881 (0.809-0.959)	0.0034	0.918 (0.806-1.05)	0.198	1.049 (0.997-1.10)	0.0656
Number of insertions (per 1 insertion)	0.870 (0.704-1.08)	0.197	0.925 (0.646-1.32)	0.669	1.012 (0.803-1.27)	0.922
Duration of ablation (per min)	1.004 (0.987-1.02)	0.272	1.007 (0.980-1.03)	0.603	0.984 (0.956-1.01)	0.273
Tumor location						
S1	NA*		2.55 (0.450-14.4)	0.290	3.300 (1.19-9.09)	0.0209
S2	0.397 (0.074-2.13)	0.282	NA*		0.913 (0.314-2.65)	0.868
S3	0.275 (0.051-1.48)	0.133	0.414 (0.055-3.09)	0.390	0.790 (0.250-2.45)	0.683
S4	0.979 (0.429-2.23)	0.959	1.350 (0.490-3.68)	0.558	1.051 (0.406-2.72)	0.917
S5	1.290 (0.629-2.65)	0.487	0.405 (0.054-3.03)	0.379	1.039 (0.422-2.55)	0.934
S6	0.698 (0.298-1.64)	0.408	0.263 (0.033-2.08)	0.206	1.120 (0.496-2.52)	0.789
S7	1.770 (1.01-3.09)	0.0449	2.31 (1.19-4.48)	0.014	1.240 (0.553-1.87)	0.597
S8	1.028 (0.597-1.77)	0.919	1.44 (0.88-2.35)	0.144	1.011 (0.993-1.08)	0.972

*There was no event with tumors at this location.
CI indicates confidence interval; NA, not available; OR, odds ratio.

particular, an upward tilt during needle puncture is likely to injure the intercostal arteries, which run on the lower edge of the ribs. However, ablation of tumors in S7 often requires this position. It is advisable to minimize the upward tilt of the needle puncture by keeping patients in a head-up position and using techniques such as artificial pleural effusion.[27] Once hemothorax occurs, the respiratory condition may deteriorate rapidly. Acute respiratory distress syndrome may occur and the resulting thrombocytopenia can aggravate the hemorrhage. In addition to stabilizing the circulation by using infusion and transfusion, thoracic drainage is often required to stabilize the respiratory condition and prevent subsequent acute respiratory distress syndrome. If the estimated blood loss was < 300 to 400 mL, we performed thoracentesis, whereas if the estimated loss exceeded 500 mL, we performed a tube thoracostomy.[28]

Hemobilia is caused by simultaneously puncturing a bile duct and a blood vessel. Regardless of the volume of hemorrhage, hemobilia may cause obstructive jaundice, resulting in potentially fatal acute obstructive suppurative cholangitis. As the hepatic artery, portal vein, and intrahepatic bile duct run together, it is important to avoid bile ducts during needle insertion. As bile ducts are visualized most easily with ultrasonography, the quality of the ultrasound device may affect the risk of hemobilia. The risk of hemobilia was the greatest with tumors in S1, which is the deepest portion of the liver and probably associated with the highest risk of penetrating intrahepatic bile ducts during needle insertion. Once hemobilia occurred, the indications for and timing of bile duct drainage is essential. A delay in commencing drainage may result in severe obstructive jaundice and liver failure, whereas we suspect that unnecessarily early drainage may delay hemostasis and increase the risk of retrograde infection.[29] Provisionally, we have set the indication criterion for bile duct drainage at bilirubin concentrations exceeding 4 mg/dL. With this strategy, we encountered no case of liver failure after hemobilia in this series.

As hemorrhagic complications after RFA are uncommon, few institutions have enough data to analyze their characteristics, risk factors, and plausible management. In

this study, we found that a low platelet count, large tumor size, and tumor location were significant risk factors for hemorrhagic complications. In addition, the experience of the operators and the quality of imaging devices affected the risk of hemorrhagic complications. Referral to a high-volume center may be the best risk management strategy for technically difficult cases. Importantly, hemorrhagic complications may often manifest more than 8 hours after the procedure. Therefore, RFA performance on inpatient basis is highly recommended.

REFERENCES

1. Rossi S, Di Stasi M, Buscarini E, et al. Percutaneous RF interstitial thermal ablation in the treatment of hepatic cancer. AJR Am J Roentgenol. 1996;167:759–768.
2. Solbiati L, Goldberg SN, Ierace T, et al. Hepatic metastases: percutaneous radio-frequency ablation with cooled-tip electrodes. Radiology. 1997;205:367–373.
3. Goldberg SN, Solbiati L, Hahn PF, et al. Large-volume tissue ablation with radio frequency by using a clustered, internally cooled electrode technique: laboratory and clinical experience in liver metastases. Radiology. 1998;209:371–379.
4. Livraghi T, Goldberg SN, Lazzaroni S, et al. Small hepatocellular carcinoma: treatment with radio-frequency ablation versus ethanol injection. Radiology. 1999;210:655–661.
5. Tateishi R, Shiina S, Teratani T, et al. Percutaneous radio-frequency ablation for hepatocellular carcinoma. An analysis of 1000 cases. Cancer. 2005;103:1201–1209.
6. Shiina S, Teratani T, Obi S, et al. A randomized controlled trial of radiofrequency ablation with ethanol injection for small hepatocellular carcinoma. Gastroenterology. 2005;129: 122–130.
7. de Baere T, Risse O, Kuoch V, et al. Adverse events during radiofrequency treatment of 582 hepatic tumors. AJR Am J Roentgenol. 2003;181:695–700.
8. Rhim H, Yoon KH, Lee JM, et al. Major complications after radio-frequency thermal ablation of hepatic tumors: spectrum of imaging findings. Radiographics. 2003;23:123–134; discussion 134–136.
9. Mulier S, Mulier P, Ni Y, et al. Complications of radiofrequency coagulation of liver tumours. Br J Surg. 2002; 89:1206–1222.

— 84 —

10. Curley SA, Marra P, Beaty K, et al. Early and late compli-
cations after radiofrequency ablation of malignant liver tumors
in 608 patients. *Ann Surg*. 2004;239:450–458.
11. Giorgio A, Tarantino L, de Stefano G, et al. Complications
after percutaneous saline-enhanced radiofrequency ablation of
liver tumors: 3-year experience with 336 patients at a single
center. *AJR Am J Roentgenol*. 2005;184:207–211.
12. Chen MH, Yang W, Yan K, et al. Treatment efficacy of
radiofrequency ablation of 338 patients with hepatic malignant
tumor and the relevant complications. *World J Gastroenterol*.
2005;11:6395–6401.
13. Chen TM, Huang PT, Lin LF, et al. Major complications of
ultrasound-guided percutaneous radiofrequency ablations for
liver malignancies: Single center experience. *J Gastroenterol
Hepatol*. 2003;23(8 Pt 2):e445–e450.
14. Kasugai H, Osaki Y, Oka H, et al. Severe complications of
radiofrequency ablation therapy for hepatocellular carcinoma:
an analysis of 3891 ablations in 2614 patients. *Oncology*.
2007;72 (suppl 1):72–75.
15. Imamura J, Tateishi R, Shiina S, et al. Neoplastic seeding after
radiofrequency ablation for hepatocellular carcinoma. *Am J
Gastroenterol*. 2008;103:3057–3062.
16. Rhim H. Complications of radiofrequency ablation in hepa-
tocellular carcinoma. *Abdom Imaging*. 2005;30:409–418.
17. Eisele RM, Schumacher G, Jonas S, et al. Radiofrequency
ablation prior to liver transplantation: focus on complications
and on a rare but severe case. *Clin Transplant*. 2008;22:20–28.
18. Ma K, Min C, Ian HX, et al. Prevention and cure of
complications from multiple-electrode radiofrequency treat-
ment of liver tumors. *Dig Dis*. 2001;19:364–366.
19. Choi H, Loyer EM, DuBrow RA, et al. Radio-frequency
ablation of liver tumors: assessment of therapeutic response
and complications. *Radiographics*. 2001;21 (Spec No):S41–S54.
20. Teratani T, Yoshida H, Shiina S, et al. Radiofrequency
ablation for hepatocellular carcinoma in so-called high-risk
locations. *Hepatology*. 2006;43:1101–1108.
21. Goldberg SN, Grassi CJ, Cardella JF, et al. Image-guided
tumor ablation: standardization of terminology and reporting
criteria. *Radiology*. 2005;235:728–739.
22. Torzilli G, Minagawa M, Takayama T, et al. Accurate
preoperative evaluation of liver mass lesions without fine-
needle biopsy. *Hepatology*. 1999;30:889–893.
23. Edmondson HA, Steiner PE. Primary carcinoma of the liver: a
study of 100 cases among 48,900 necropsies. *Cancer*. 1954;7:
462–503.
24. Goldberg SN, Grassi CJ, Cardella JF, et al. Image-guided
tumor ablation: standardization of terminology and reporting
criteria. *J Vasc Interv Radiol*. 2005;16:765–778.
25. Couinaud C. Lobes et segments hepatiques. Note sur
l'architecture anatomique et chirurgicale du foie. *Presse Med*.
1954;62:709–711.
26. Obi S, Shiratori Y, Shiina S, et al. Early detection of haemobilia
associated with percutaneous ethanol injection for hepatocellular
carcinoma. *Eur J Gastroenterol Hepatol*. 2000;12:285–290.
27. Kondo Y, Yoshida H, Tateishi R, et al. Percutaneous
radiofrequency ablation of liver cancer in the hepatic dome
using the intrapleural fluid infusion technique. *Br J Surg*.
2008;95:996–1004.
28. Misthos P, Kakaris S, Sepsas E, et al. A prospective analysis of
occult pneumothorax, delayed pneumothorax and delayed
hemothorax after minor blunt thoracic trauma. *Eur J
Cardiothorac Surg*. 2004;25:859–864.
29. Sasahira N, Tada M, Yoshida H, et al. Extrahepatic biliary
obstruction after percutaneous tumour ablation for hepatocel-
lular carcinoma: aetiology and successful treatment with
endoscopic papillary balloon dilatation. *Gut*. 2005;54:698–702.

Molecular pathogenesis of malignant melanoma: a different perspective from the studies of melanocytic nevus and acral melanoma

Minoru Takata, Hiroshi Murata and Toshiaki Saida

Department of Dermatology, Shinshu University School of Medicine, Asahi, Matsumoto, Japan

CORRESPONDENCE Minoru Takata, e-mail: mtakata@shinshu-u.ac.jp

Summary

The Clark model for melanoma progression emphasizes a series of histopathological changes beginning from benign melanocytic nevus to melanoma via dysplastic nevus. Several models of the genetic basis of melanoma development and progression are based on this Clark's multi-step model, and predict that the acquisition of a *BRAF* mutation can be a founder event in melanocytic neoplasia. However, our recent investigations have challenged this view, showing the polyclonality of *BRAF* mutations in melanocytic nevi. Furthermore, it is suggested that many melanomas, including acral and mucosal melanomas, arise *de novo*, not from melanocytic nevus. While mutations of the *BRAF* gene are frequent in melanomas on non-chronic sun damaged skin which are prevalent in Caucasians, acral and mucosal melanomas harbor mutations of the *KIT* gene as well as the amplifications *of cyclin D1* or *cyclin-dependent kinase 4* gene. Amplifications of the *cyclin D1* gene are detected in normal-looking 'field melanocytes', which represent a latent progression phase of acral melanoma that precedes the stage of atypical melanocyte proliferation in the epidermis. Based on these observations, we propose an alternative genetic progression model for melanoma.

Classification systems of melanoma: Clark, Ackerman, and Bastian

Clark's classification of malignant melanoma was established in 1970s, which distinguishes four main types of melanoma; superficial spreading melanoma (SSM), lentigo maligna melanoma (LMM), nodular melanoma (NM), and acral lentiginous melanoma (ALM) (Clark et al., 1979). This classification has been widely used both by clinicians and researchers, and the current World Health Organization (WHO) classification of skin tumors is based on this classification (LeBoit et al., 2006). These distinctions, based on the microscopic growth patterns, are associated with clinical features such as anatomic site of primary tumor and patient age.

However, Ackerman (1980) questioned the existence of biologically distinct melanoma types, and proposed a unifying concept of melanoma. He maintained that all melanomas evolve in a similar way, at first spread

horizontally within the epidermis and eventually extend vertically into the dermis, and that the morphological differences are entirely secondary to the anatomic site in which the tumor arises. In case of NM, morphological differences may be a consequence of differences in the pace of tumor evolution; i.e., the vertical growth phase simply supervenes upon a briefer horizontal growth phase. In fact, the impact of Clark's classification on clinical management is limited, because no significant difference in overall survival could be demonstrated between the categories when tumors of equivalent thickness were compared (Balch et al., 2000).

Recently, in their effort to integrate clinicopathological features with somatic genetic alterations, Boris Bastian and his colleagues proposed a new classification system of melanoma (Curtin et al., 2005). They described distinct pattern of chromosomal aberrations and mutations in the oncogenes such as *BRAF*, *NRAS* and *KIT*, which correlated with the site of primary tumor and the degree

of chronic sun-induced damage of the surrounding skin. Based on these observations, they classified melanomas into four groups; melanoma on skin with chronic sun-damage (CSD melanoma), melanoma on skin without chronic sun-damage (non-CSD melanoma), melanoma on palms, soles and nail bed (acral melanoma), and melanoma on mucous membrane (mucosal melanoma). Non-CSD melanoma roughly corresponds to SSM in the Clark's classification, CSD melanoma to LMM, and acral melanoma to ALM. NM was excluded in this new classification system, because NMs may arise any anatomical site and do not have unique genetic features that justify regarding them as a unique type.

Non-CSD melanomas are characterized by high frequency of BRAF mutations (reaching up to 75%), while other three types, i.e., CSD, acral and mucosal melanomas show a low frequency of BRAF mutation (Curtin et al., 2005; Maldonado et al., 2003). Instead, these types of melanoma show aberrations in other genes, such as mutations and/or amplifications of receptor tyrosine kinase KIT (Curtin et al., 2006), as well as amplifications of cyclin D1 (CCND1) and cyclin-dependent kinase 4 (CDK4) genes that regulate cell-cycle progression (Bastian et al., 2000; Curtin et al., 2005). Such a difference of genetic alterations indicates distinct genetic pathways in the development of melanoma depending on the anatomical site of the primary lesion.

The new classification system by Bastian's group appears to support the Clark's classification, confirming the existence of genetically distinct subsets in melanomas. However, it is not necessarily contradictory to Ackerman's unifying concept that suggested the relationship between morphological difference and the anatomical site of the primary tumor. Although the Bastian's classification somewhat reflects somatic genetic changes of individual tumors, categorization of melanoma types still depends on the anatomical site of the primary tumors and microscopic morphological criteria grading solar elastosis of the dermis surrounding the tumors. In the future, more refined classification systems based solely on molecular analyses or those integrating genetic and morphologic features, such as the one recently reported by Bastian's group (Viros et al., 2008), are necessary, which will be able to provide relevant information for selecting treatments for patients with distant metastasis.

Genetic basis of melanoma evolution and progression based on the Clark model

In addition to the classification system, Clark et al. (1984) also proposed a multi-step progression model of melanoma. The theory comes from clinical and histopathological observations in sporadic melanomas (mostly non-CSD melanomas) as well as in familiar melanomas

in dysplastic nevus syndrome patients (Clark et al., 1978), all of which are prevalent in Caucasians. Several models of the genetic basis of melanoma development
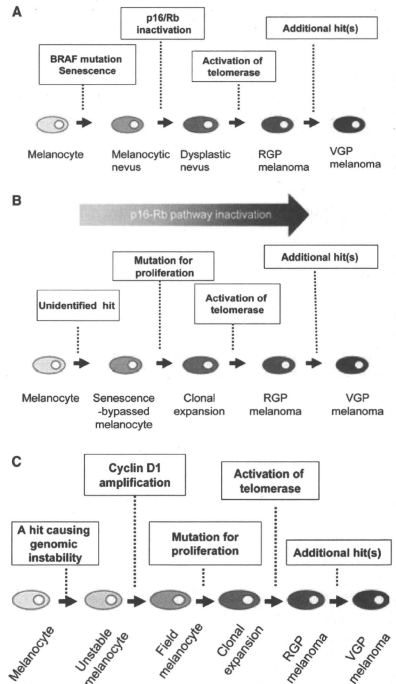

Figure 1. (A) A genetic model of melanoma development and progression based on the Clark model (adopted from Bennett, 2003; and Miller and Mihm, 2006). This model emphasizes a series of histopathological changes beginning from benign melanocytic nevus to melanoma via dysplastic nevus, and predicts that BRAF mutation is a crucial step of initiation of melanocytic neoplasia. Progression from benign melanocytic nevus to dysplastic nevus requires escape from senescence mediated through p16[INK4a]-Rb pathway inactivation. (B) A genetic model of de novo melanoma development (adopted from Michaloglou et al. 2008) with modifications). The first event would be an unidentified hit, which might collaborate with inactivation of p16[INK4a]-Rb pathway. When a melanocyte already suffering from this hit acquires a proliferative mutation, such as BRAF[V600E], it might fail to undergo oncogene-induced senescence and clonally proliferate. (C) A hypothetical genetic progression model of acral melanoma. Normal melanocytes, which acquired genomic instability and CCND1 amplification give rise to field cells, the precursors of RGP melanoma. Progression from field cells to RGP melanoma may require mutations for proliferation, such as KIT, and immortalization. RGP, radial growth phase; VGP, vertical growth phase.

and progression are based on this Clark's multi-step model, which has been universal in the melanoma research community (Bennett, 2003; Michaloglou et al., 2008; Miller and Mihm, 2006) (Figure 1A).

According to these models, the first phenotypic change in normal melanocytes is the development of benign melanocytic nevus. Melanocytic nevus can be regarded as the benign counterpart of melanoma, and may occasionally give rise to melanoma. Like melanoma, melanocytic nevus frequently harbor activating *BRAF* mutations (Pollock et al., 2003), which are thought to be an initial step in melanocytic neoplasia; however, the initial growth of melanocytic nevus is followed by stabilization of the size and loss of most proliferative activity. Two recent studies show that sustained *BRAF*^{V600E} expression in normal human melanocytes induces cell-cycle arrest accompanied by the induction of both p16^{INK4a} and acidic β-galactosidase activity, which are also demonstrated in lesions of melanocytic nevus in situ (Gray-Schopfer et al., 2006; Michaloglou et al., 2005). Moreover, a mouse model of melanocytic nevus and melanoma, which is driven by the inducible expression of BRAF^{V600E} in melanocytes, has been developed recently, providing further evidence that the acquisition of a *BRAF* mutation can be a founder event in melanocyte transformation (Dhomen et al., 2009). Thus, it is suggested that melanocytic nevus is a benign clonal tumor, which temporarily undergoes proliferation via oncogenic *BRAF* signaling followed by growth arrest due to oncogene-induced senescence (Michaloglou et al., 2008).

The next step toward melanoma evolution is dysplastic nevus, which histopathologically shows structural and cytological atypia. Dysplastic nevus may arise from a preexisting melanocytic nevus or as a new lesion. The molecular abnormality at this stage of progression may be disruption of p16^{INK4a}-retinoblastoma (Rb) pathway, mostly by the inactivation of *CDKN2A*, a gene encoding p16^{INK4a} and p19^{ARF}, because 25–40% of patients with familial melanoma, who also develop multiple dysplastic nevi, have germline mutations of *CDKN2A* (Hussussian et al., 1994). Frequent loss of heterozygosity at the *CDKN2A* locus, and occasional mutations in the *CDKN2A* gene were actually demonstrated in sporadic dysplastic nevi (Lee et al., 1997).

The third step in progression is the radial growth phase (RGP) melanoma, which spreads progressively within or just beneath the epidermis. In this phase of progression, neoplastic melanocytes are immortal, which can be achieved by activation of human telomerase reverse transcriptase (hTERT). Deficiency in the p16^{INK4a}-Rb pathway as well as hTERT activation appears necessary for melanocyte immortalization, and p16^{INK4a}-deficient human melanocytes show a high rate of apoptosis that is suppressed by keratinocytes or their products (Sviderskaya et al., 2003). Thus, it is speculated that RGP melanoma cells require keratinocytes or

their products for survival, and can grow only in or near the epidermis.

The final stage in melanoma progression is the vertical growth phase (VGP), which grows deep in the dermis and is metastasis competent. For progression to the VGP, mutations repressing apoptosis would be required, which allow cells to survive in the absence of keratinocytes. These include PTEN loss, which would inhibit apoptosis via AKT activation, over-expression of a number of protein kinases or RAS activation, and β-catenin activation [reviewed in Bennett (2003)]. Progression from RGP to VGP is also marked by the loss of E-cadherin, as well as the aberrant expression of N-cadherin and $\alpha V \beta 3$ integrin [reviewed in Miller and Mihm (2006)]. In addition, interaction between melanoma cells and stromal fibroblasts is important, creating a context that promotes tumor growth, migration, and angiogenesis [reviewed in Li et al. (2003)].

Polyclonality of *BRAF* mutations in melanocytic nevi: challenging the Clark model

If melanocytic nevus is a senescent clone of melanocytes that acquire *BRAF* mutations, as suggested by the Clark model of melanoma progression, all nevus cells within the lesions of melanocytic nevus should be *BRAF* mutants (Michaloglou et al., 2008) (Figure 2A); however, this is not the case. We have recently examined the clonality of melanocytic nevus using *BRAF* mutation as a molecular marker (Lin et al., 2009). This idea stems from our previous study examining *BRAF* mutations in a large series of melanocytic nevi excised from different anatomical sites. In the study, detection rates of *BRAF* mutations in melanocytic nevi were markedly different between direct sequencing and the more sensitive shifted termination assay, suggesting that minor populations of nevus cells with *BRAF*
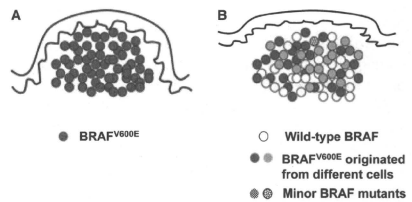
● BRAF^{V600E} ○ Wild-type BRAF

● ● BRAF^{V600E} originated
      from different cells

◉ ◉ Minor BRAF mutants

Figure 2. Histogenesis models of melanocytic nevus. (A) If melanocytic nevus is a benign clonal tumor, which temporarily undergo proliferation via oncogenic *BRAF* signaling followed by growth arrest due to oncogene-induced senescence, all the nevus cells within a lesion should be BRAF mutants. (B) However, actual lesions of melanocytic nevus consist of cells with wild-type BRAF as well as BRAF mutated-nevus cells of multi-cellular origin.

mutations were admixed with *BRAF* wild-type nevus cells in these lesions (Ichii-Nakato et al., 2006). In a follow-up study (Lin et al., 2009), using immunomagnetic cell isolation or laser-capture microdissection procuring single nevus cells, we actually demonstrated nevus cells that contained wild-type *BRAF* mixed with nevus cells that contained *BRAF* ^{V600E} within a lesion of acquired melanocytic nevus. Rare *BRAF* mutations, such as *BRAF*^{V600A} and *BRAF*^{T599I}, which had been reported in melanomas, were also identified. Furthermore, we showed that nevus cells harboring the same *BRAF*^{V600E} mutation originated from different cells. This rather surprising finding was obtained by an elegant strategy of subcloning and sequencing long-range PCR products encompassing both *BRAF* exon 15 and a neighboring single-nucleotide polymorphism (SNP) rs7801086, using four nevus tissues excised from patients who were G/T heterozygotes for this SNP. We found that bacterial subclones harboring the *BRAF*^{V600E} mutation were accompanied by both the G SNP and the T SNP. These results clearly indicate the polyclonality of *BRAF* mutations in acquired melanocytic nevi (Figure 2B), and contradict the current models predicting BRAF mutation as a founder even in melanocytic neoplastic progression (Dhomen et al., 2009; Michaloglou et al., 2008). The potential caveat of our study is that we examined only a small number of nevi which were mostly Unna's nevi and Miescher's nevi. We did not examine Clark's nevi, which are most common in adult Caucasians and are sometimes seen in association with melanoma. However, we have observed similar polyclonality of BRAF mutations in primary melanomas (Lin et al., unpublished observation).

Nevertheless, our observations raise a number of interesting and important questions. Are melanocytic nevi (and perhaps many other benign lesions in skin as well as in many other tissues) monoclonal or polyclonal? Are melanomas really derived from a single melanocyte that acquired oncogenic mutations? What is the crucial mutation that causes initial clonal proliferation of melanocytes? These questions should be addressed in future studies.

De novo melanoma and its progression model

While the Clark model of melanoma evolution was prevailing, a few investigators have maintained that most primary melanomas arise *de novo*, not associated with melanocytic nevus, because the majority of melanoma emerge in normal skin, not in association with dysplastic nevus, even in patients with familial dysplastic nevus syndrome (Ackerman and Mihara, 1985). From the clinical and histopathological observations in acral melanoma and mucosal melanoma, we also believe that all melanoma, at least of these subtypes, arise *de novo* (Saida, 1994). Recently, it is suggested that melanoma arises

from divergent pathways, and that many melanomas arise *de novo* whereas some may arise from pre-exsisting melanocytic nevi (Rivers, 2004). Thus, the current molecular models of melanoma development, based on the Clark's model may not be applied to these *de novo* melanomas, and an alternative model is necessary.

Michaloglou et al. (2008) speculated that the first event in *de novo* melanoma development would be a yet unidentified hit, which may enable melanocytes to escape from oncogene-induced senescence (Figure 1B). This initial hit might collaborate with p16^{INK4a}-Rb inactivation, which could be achieved by deletion, mutation or promoter methylation of the *CDKN2A* gene, amplification of *CCND1* or *CDK4*, or Rb mutation [reviewed in Bennett (2008)]. Although loss of p16^{INK4a} expression was reported to be a late event in melanoma progression (Reed et al., 1995), transcriptional repression of p16^{INK4a} by ID1 was demonstrated in early in situ melanomas (Polsky et al., 2001). When a melanocyte already suffering from this hit acquires a proliferative mutation such as BRAF^{V600E}, it may fail to undergo oncogene-induced senescence and clonally proliferate. Thus, it is possible that the order of somatic genetic changes may determine whether a melanoma originates from a nevus or *de novo*. To gain immortality, proliferating melanocytes have to overcome replicative senescence by inactivating p16^{INK4a}-Rb pathway and by maintaining a minimum telomere length, which can be achieved by activation of hTERT. If inactivation of p16^{INK4a}-Rb had occurred earlier, this step could be achieved by hTERT activation alone. Finally, full oncogenic transformation to VGP melanoma may require additional genetic or epigenetic hits. These would include mutations suppressing apoptosis, changes of adhesion molecule, and up-regulation of growth factors, as discussed in the Clark model.

However, this model of *de novo* melanoma formation is only speculative. Recent advances in understanding molecular pathogenesis of acral melanoma and mucosal melanoma may provide additional insights into a molecular model of *de novo* melanoma development. The key somatic genetic alterations in acral and mucosal melanomas so far identified are *KIT* mutations and *CCND1* amplifications.

KIT mutations in acral and mucosal melanomas

KIT encodes a receptor tyrosine kinase, whose ligand is a stem cell factor (SCF). The dysregulation of KIT is thought to play a role in certain neoplastic disorders, including systemic mastocytosis, acute myelogenous leukemia, germ cell tumors, and gastrointestinal stromal cell tumors [reviewed in Patnaik et al. (2007)]. KIT–SCF signaling is also essential for melanocyte development, differentiation, proliferation, survival and migration [reviewed in Wehrle-Haller (2003)]. While KIT

expression is found in normal melanocytes, benign melanocytic nevi and in situ melanomas, it appears to be down-regulated in invasive and metastatic melanomas (Montone et al., 1997; Natali et al., 1992). Furthermore, activating *KIT* mutation was rare, found in only 3 of 153 melanomas in one large-scale study (Willmore-Payne et al., 2006). Based on these obsevations, *KIT* was formerly dismissed as not acting as a melanoma oncogene.

However, a recent study by Curtin et al. (2006) has highlighted the important role of *KIT* in a subset of melanomas. These authors examined 102 primary melanomas excised from various anatomical sites, and found mutations and/or copy number increases of *KIT* in 39% of mucosal melanomas, 36% of acral melanomas and 28% of CSD melanomas. By contrast, none of the non-CSD melanomas, which are the predominant type of melanomas in Caucasians, had *KIT* aberrations. The result indicates that the former ignorance of *KIT* was due to selection bias of only examining particular melanoma types. Several follow-up studies (Antonescu et al., 2007; Beadling et al., 2008; Rivera et al., 2008), including one from our own laboratory (Ashida et al., 2009), have confirmed rather frequent *KIT* mutations and/or amplifications in acral and mucosal melanomas. Furthermore, in vitro studies have shown significant growth suppressive effects of small molecular inhibitors targeting KIT, such as imatinib and sunitinib, in melanoma cell lines harboring *KIT* mutations (Ashida et al., 2009; Jiang et al., 2008). Because KIT activity constitutes the major signaling node involved in growth and survival, treatment of KIT-targeting drugs lead to the simultaneous inhibition of the mitogen-activated protein kinase (MAPK), phosphatidyl-inositol-3-kinase (PI3K)/Akt, and janus kinase (JAK)/signal transducer and activation of transcription (STAT) signaling pathways, as well as cell-cycle arrest and apoptosis (Jiang et al., 2008). Dramatic clinical effects of imatinib have actually been seen in mucosal melanoma patients with documented *KIT* activating mutations (Hodi et al., 2008; Lutzky et al., 2008). These observations indicate that *KIT* is an important oncogene and a critical target in melanomas arising on acral skin and mucosa.

CCND1 gene amplifications in acral melanoma

Together with MAPK and PI3K/Akt activation, the p16[INK4a]-CCND1-CDK4-Rb pathway is functionally altered in most melanomas (Bartkova et al., 1996). CCND1 positively regulates the activity of CDKs, leading to phosphorylation of Rb and promoting entry into mitosis. The *CCND1* gene is an oncogene, rearranged and activated in centrocytic lymphoma and parathyroid cancers, and amplified and over-expressed in various human cancers [reviewed in Tashiro et al. (2007)].

Although the role of CCND1 was less well established in meloma, recent studies have revealed frequent amplifications (~45%) of the *CCND1* gene in acral melanoma (Bastian et al., 2000; Sauter et al., 2002; Takata et al., 2005). Interestingly, while gene amplifications are usually found in association with disease progression in other cancers, *CCND1* gene amplifications in acral melanoma are detected early in the RGP of primary melanoma (Bastian et al., 2000) and in the intraepidermal melanocytes in very early acral melanoma in situ lesions, in which only a slight increase of non-atypical melanocytes in the basal cell layer of the epidermis was observed (Yamaura et al., 2005). Furthermore, copy number increase of *CCND1* gene was observed even in normal-looking melanocytes in the epidermis beyond the histopathologically recognizable margin of melanoma (Bastian et al., 2000; North et al., 2008). These genetically aberrant cells with normal morphology are "field cells" (Bastian, 2003), which represent a latent progression phase that precedes the stage of melanocyte proliferation in the epidermis. Such field cells in acral melanoma extend from a few to 10 mm beyond the histopathological margin, and the extent does not correlate with tumor depth or diameter (North et al., 2008). These observations suggest that amplification of the *CCND1* gene might be one of the earliest events in melanoma development in glabrous skin. The presence of amplifications, however, indicates that other aberrations likely cause genomic instability (North et al., 2008). The progressive increase of the *CCND1* copy number from normal-looking melanocytes to the in situ portion to the invasive melanoma was observed, suggesting that the increased *CCND1* gene dosage confers a growth advantage during tumor progression (North et al., 2008); however, this may simply reflect the increase of genomic instability associated with melanoma progression.

To further explore the molecular events in the initiation of acral melanoma, we have succeeded in establishing a novel cell line, SMYM-PRGP, from a RGP of acral melanoma (Murata et al., 2007). Reflecting the characteristic of early melanoma cells, SMYM-PRGP is not tumorigenic in vivo and shows growth-factor dependency, especially for endothelin-1, a known potent growth factor for normal melanocytes (Imokawa et al., 1992). While it shows neither *NRAS* nor *BRAF* mutations, SMYM-PRGP harbors focal amplifications of *CCND1* and *hTERT* genes. The CCND1 protein level is about 10 times higher than that of normal melanocytes. Thus, instead of *NRAS* or *BRAF* mutations, *CCND1* amplification may be a crucial genetic change, which induces the proliferation of SMYM-PRGP cells through the endothelin signaling; however, upon stimulation with endothelin -1, although CCND1 protein levels increased, phosphorylation of Rb protein did not increase, suggesting that over-expression of CCND1 protein may have little effect on cell-cycle

progression but may act as a survival factor in an early stage of acral melanoma evolution (Murata et al., 2007).

This particular cell line also provides insights into the immortalization of melanocytes. Previous investigations indicate that both deficiency of the $p16^{INK4a}$-Rb pathway and telomere maintenance are required for immortalization of human melanocytes (Sviderskaya et al., 2002). While SMYM-PRGP cells harbor amplifications of the $hTERT$ gene, and show increased telomerase activity, they express $p16^{INK4a}$ protein at a level equal to that of normal melanocytes (Murata et al., 2007). Thus, there is a different mechanism which coordinates with hTERT in melanocyte immortalization. This could be the overexpression of CCND1 protein caused by gene amplification, since it may disrupt the $p16^{INK4a}$-Rb pathway by increasing CCND1-CDK4/6 complexes. It is also suggested that $CDK4$ amplification may obviate the need for $p16^{INK4a}$ inactivation (Curtin et al., 2005).

A hypothetical molecular model of acral melanoma development

We propose a hypothetical genetic model of acral melanoma (Figure 1C). The earliest genetic alteration so far identified in acral melanoma is the amplification of $CCND1$, which are detected in the very early lesions of acral melanoma in situ (Yamaura et al., 2005); however, this could not be the initial genetic alteration, but rather represents genomic instability, because gene amplification requires recurrent double-stranded DNA breaks (North et al., 2008). Thus, the first genetic aberration affecting normal melanocytes in acral volar skin would be one that disrupts the maintenance of genomic integrity, for instance, failure of the cell-cycle checkpoint [reviewed in Dash and El-Deiry (2004)]. Melanocytes harboring the amplification of $CCND1$ may be selected for clonal expansion. While the oncogene amplification would lead to cell proliferation, it may act as a survival factor as well, as suggested in the study of SMYM-PRGP cells (Murata et al., 2007). Then, acquiring activating mutations in oncogenes, such as KIT (Curtin et al., 2006), may be a crucial step inducing proliferation of 'field melanocytes'. Because inactivation of $p16^{INK4a}$-Rb pathway is already accomplished by the $CCND1$ amplification in 'field melanocytes', they could overcome oncogene-induced senescence. The proliferating melanocytes should also be immortal by extending telomeres, which is usually through activation of the expression of telomerase by the up-regulation of hTERT. Although RGP melanoma cells are immortal, they are not tumorigenic and are dependent on growth factors secreted from keratinocyte, such as endothelin-1 (Murata et al., 2007). The final step from RGP to VGP may be mediated by similar genetic or phenotypic alterations discussed in the Clark model and the de novo melanoma model.

Concluding remarks

Most of the published studies on melanoma to date have been from the United States, Europe and Australia, and the cell lines and clinical samples used in these studies were mostly non-CSD melanomas obtained from Caucasian patients; however, as discussed in this review, there are clear differences in the genetic alterations among different types of melanomas. Thus, our current knowledge about the pathogenesis of melanoma may have been biased by examining only one particular melanoma type, i.e., non-CSD melanomas. Investigations of acral melanomas and mucosal melanomas have revealed the importance of KIT and $CCND1$ genes in the development of these types of melanoma, and will help us to develop effective treatment strategies depending on the type of melanoma. More importantly, investigations of these subtypes provide deeper insights into the molecular pathogenesis of melanoma and also of other cancers in general.

Acknowledgements

References

Ackerman, A.B. (1980). Malignant melanoma: a unifying concept. Hum. Pathol. 11, 591–595.

Ackerman, A.B., and Mihara, I. (1985). Dysplasia, dysplastic melanocytes, dysplastic nevi, the dysplastic nevus syndrome, and the relation between dysplastic nevi and malignant melanoma. Hum. Pathol. 16, 87–91.

Antonescu, C.R., Busam, K.J., Francone, T.D. et al. (2007). L576P KIT mutation in anal melanomas correlates with KIT protein expression and is sensitive to specific kinase inhibition. Int. J. Cancer 121, 257–264.

Ashida, A., Takata, M., Murata, H., Kido, K., and Saida, T. (2009). Pathological activation of KIT in metastatic tumors of acral and mucosal melanomas. Int. J. Cancer 124, 862–868.

Balch, C.M., Buzaid, A.C., Atkins, M.B. et al. (2000). A new American Joint Committee on Cancer staging system for cutaneous melanoma. Cancer 88, 1484–1491.

Bartkova, J., Lukas, J., Guldberg, P., Alsner, J., Kirkin, A.F., Zeuthen, J., and Bartek, J. (1996). The p16-cyclin D/Cdk4-pRb pathway as a functional unit frequently altered in melanoma pathogenesis. Cancer Res. 56, 5475–5483.

Bastian, B.C. (2003). Understanding the progression of melanocytic neoplasia using genomic analysis: from fields to cancer. Oncogene 22, 3081–3086.

Bastian, B.C., Kashani-Sabet, M., Hamm, H., Godfrey, T., Moore, 2nd D.H., Brocker, E.B., LeBoit, P.E., and Pinkel, D. (2000). Gene amplifications characterize acral melanoma and permit the detection of occult tumor cells in the surrounding skin. Cancer Res. 60, 1968–1973.

Beadling, C., Jacobson-Dunlop, E., Hodi, F.S. et al. (2008). KIT gene mutations and copy number in melanoma subtypes. Clin. Cancer Res. 14, 6821–6828.

Bennett, D.C. (2003). Human melanocyte senescence and melanoma susceptibility genes. Oncogene 22, 3063–3069.

Bennett, D.C. (2008). How to make a melanoma: what do we know of the primary clonal events? Pigment Cell Melanoma Res. 21, 27–38.

Clark Jr, W.H., Reimer, R.R., Greene, M., Ainsworth, A.M., and Mastrangelo, M.J. (1978). Origin of familial malignant melanomas from heritable melanocytic lesions. 'The B-K mole syndrome'. Arch. Dermatol. 114, 732–738.

Clark Jr, W.H., and Mastrangelo, M.J. (1979). Human malignant melanoma. New York (USA): Grune & Stratton.

Clark Jr, W.H., Elder, D.E., Guerry, D.t., Epstein, M.N., Greene, M.H., and Van Horn, M. (1984). A study of tumor progression: the precursor lesions of superficial spreading and nodular melanoma. Hum. Pathol. 15, 1147–1165.

Curtin, J.A., Fridlyand, J., Kageshita, T. et al. (2005). Distinct sets of genetic alterations in melanoma. N. Engl. J. Med. 353, 2135–2147.

Curtin, J.A., Busam, K., Pinkel, D., and Bastian, B.C. (2006). Somatic activation of KIT in distinct subtypes of melanoma. J. Clin. Oncol. 24, 4340–4346.

Dash, B.C., and El-Deiry, W.S. (2004). Cell cycle checkpoint control mechanisms that can be disrupted in cancer. Methods Mol. Biol. 280, 99–161.

Dhomen, N., Reis-Filho, J.S., da Rocha Dias, S., Hayward, R., Savage, K., Delmas, V., Larue, L., Pritchard, C., and Marais, R. (2009). Oncogenic Braf induces melanocyte senescence and melanoma in mice. Cancer Cell 15, 294–303.

Gray-Schopfer, V.C., Cheong, S.C., Chong, H., Chow, J., Moss, T., Abdel-Malek, Z.A., Marais, R., Wynford-Thomas, D., and Bennett, D.C. (2006). Cellular senescence in naevi and immortalisation in melanoma: a role for p16? Br. J. Cancer 95, 496–505.

Hodi, F.S., Friedlander, P., Corless, C.L. et al. (2008). Major response to imatinib mesylate in KIT-mutated melanoma. J. Clin. Oncol. 26, 2046–2051.

Hussussian, C.J., Struewing, J.P., Goldstein, A.M., Higgins, P.A., Ally, D.S., Sheahan, M.D., Clark Jr, W.H., Tucker, M.A., and Dracopoli, N.C. (1994). Germline p16 mutations in familial melanoma. Nat. Genet. 8, 15–21.

Ichii-Nakato, N., Takata, M., Takayanagi, S., Takashima, S., Lin, J., Murata, H., Fujimoto, A., Hatta, N., and Saida, T. (2006). High frequency of BRAFV600E mutation in acquired nevi and small congenital nevi, but low frequency of mutation in medium-sized congenital nevi. J. Invest. Dermatol. 126, 2111–2118.

Imokawa, G., Yada, Y., and Miyagishi, M. (1992). Endothelins secreted from human keratinocytes are intrinsic mitogens for human melanocytes. J. Biol. Chem. 267, 24675–24680.

Jiang, X., Zhou, J., Yuen, N.K. et al. (2008). Imatinib targeting KIT-mutant oncoprotein in melanoma. Clin. Cancer Res. 14, 7726–7732.

LeBoit, P.E., Burg, G., Weedon, D., and Sarasin, A. (2006). Skin tumours. Pathology and genetics. Lyon (France): IARCPress.

Lee, J.Y., Dong, S.M., Shin, M.S. et al. (1997). Genetic alterations of p16INK4a and p53 genes in sporadic dysplastic nevus. Biochem. Biophys. Res. Commun. 237, 667–672.

Li, G., Satyamoorthy, K., Meier, F., Berking, C., Bogenrieder, T., and Herlyn, M. (2003). Function and regulation of melanoma-stromal interactions: when seeds meet soil. Oncogene 22, 3162–3171.

Lin, J., Takata, M., Murata, H., Goto, Y., Kido, K., Ferrone, S., and Saida, T. (2009). Polyclonality of BRAF mutations in acquired melanocytic nevi. J. Natl Cancer Inst, DOI:10.1093/jnci/djp309.

Lutzky, J., Bauer, J., and Bastian, B.C. (2008). Dose-dependent, complete response to imatinib of a metastatic mucosal melanoma with a K642E KIT mutation. Pigment Cell Melanoma Res., 21, 492–493.

Maldonado, J.L., Fridlyand, J., Patel, H. et al. (2003). Determinants of BRAF mutations in primary melanomas. J. Natl Cancer Inst. 95, 1878–1890.

Michaloglou, C., Vredeveld, L.C., Soengas, M.S. et al. (2005). BRAFE600-associated senescence-like cell cycle arrest of human naevi. Nature 436, 720–724.

Michaloglou, C., Vredeveld, L.C., Mooi, W.J., and Peeper, D.S. (2008). BRAF(E600) in benign and malignant human tumours. Oncogene 27, 877–895.

Miller, A.J., and Mihm Jr, M.C. (2006). Melanoma. N. Engl. J. Med. 355, 51–65.

Montone, K.T., van Belle, P., Elenitsas, R., and Elder, D.E. (1997). Proto-oncogene c-kit expression in malignant melanoma: protein loss with tumor progression. Mod. Pathol. 10, 939–944.

Murata, H., Ashida, A., Takata, M., Yamaura, M., Bastian, B.C., and Saida, T. (2007). Establishment of a novel melanoma cell line SMYM-PRGP showing cytogenetic and biological characteristics of the radial growth phase of acral melanomas. Cancer Sci. 98, 958–963.

Natali, P.G., Nicotra, M.R., Winkler, A.B., Cavaliere, R., Bigotti, A., and Ullrich, A. (1992). Progression of human cutaneous melanoma is associated with loss of expression of c-kit proto-oncogene receptor. Int. J. Cancer 52, 197–201.

North, J.P., Kageshita, T., Pinkel, D., Leboit, P.E., and Bastian, B.C. (2008). Distribution and significance of occult intraepidermal tumor cells surrounding primary melanoma. J. Invest. Dermatol. 128, 2024–2030.

Patnaik, M.M., Tefferi, A., and Pardanani, A. (2007). Kit: molecule of interest for the diagnosis and treatment of mastocytosis and other neoplastic disorders. Curr Cancer Drug Targets 7, 492–503.

Pollock, P.M., Harper, U.L., Hansen, K.S. et al. (2003). High frequency of BRAF mutations in nevi. Nat. Genet. 33, 19–20.

Polsky, D., Young, A.Z., Busam, K.J., and Alani, R.M. (2001). The transcriptional repressor of p16/Ink4a, Id1, is up-regulated in early melanomas. Cancer Res. 61, 6008–6011.

Reed, J.A., Loganzo Jr, F., Shea, C.R. et al. (1995). Loss of expression of the p16/cyclin-dependent kinase inhibitor 2 tumor suppressor gene in melanocytic lesions correlates with invasive stage of tumor progression. Cancer Res. 55, 2713–2718.

Rivera, R.S., Nagatsuka, H., Gunduz, M. et al. (2008). C-kit expression correlated with activating mutations in KIT gene in oral mucosal melanoma. Virchows Arch. 452, 27–32.

Rivers, J.K. (2004). Is there more than one road to melanoma? Lancet 363, 728–730.

Saida, T. (1994). The concept of de novo origin of cutaneous malignant melanoma. Eur J Dermatol 4, 252–254.

Sauter, E.R., Yeo, U.C., von Stemm, A. et al. (2002). Cyclin D1 is a candidate oncogene in cutaneous melanoma. Cancer Res. 62, 3200–3206.

Sviderskaya, E.V., Hill, S.P., Evans-Whipp, T.J. et al. (2002). p16(Ink4a) in melanocyte senescence and differentiation. J. Natl Cancer Inst. 94, 446–454.

Sviderskaya, E.V., Gray-Schopfer, V.C., Hill, S.P. et al. (2003). p16/cyclin-dependent kinase inhibitor 2A deficiency in human melanocyte senescence, apoptosis, and immortalization: possible implications for melanoma progression. J. Natl Cancer Inst. 95, 723–732.

Takata, M., Goto, Y., Ichii, N., Yamaura, M., Murata, H., Koga, H., Fujimoto, A., and Saida, T. (2005). Constitutive activation of the mitogen-activated protein kinase signaling pathway in acral melanomas. J. Invest. Dermatol. 125, 318–322.

Tashiro, E., Tsuchiya, A., and Imoto, M. (2007). Functions of cyclin D1 as an oncogene and regulation of cyclin D1 expression. Cancer Sci. *98*, 629–635.

Viros, A., Fridlyand, J., Bauer, J., Lasithiotakis, K., Garbe, C., Pinkel, D., and Bastian, B.C. (2008). Improving melanoma classification by integrating genetic and morphologic features. PLoS Med *5*, e120.

Wehrle-Haller, B. (2003). The role of Kit-ligand in melanocyte development and epidermal homeostasis. Pigment Cell Res. *16*, 287–296.

Willmore-Payne, C., Holden, J.A., Hirschowitz, S., and Layfield, L.J. (2006). BRAF and c-kit gene copy number in mutation-positive malignant melanoma. Hum. Pathol. *37*, 520–527.

Yamaura, M., Takata, M., Miyazaki, A., and Saida, T. (2005). Specific dermoscopy patterns and amplifications of the cyclin D1 gene to define histopathologically unrecognizable early lesions of acral melanoma in situ. Arch. Dermatol. *141*, 1413–1418.

Glypican-3 expression predicts poor clinical outcome of patients with early-stage clear cell carcinoma of the ovary

Tomokazu Umezu, Kiyosumi Shibata, Hiroaki Kajiyama, Eiko Yamamoto, Akihiro Nawa, Fumitaka Kikkawa

Department of Obstetrics and Gynecology, Nagoya University Graduate School of Medicine, Nagoya, Japan

Correspondence to
Tomokazu Umezu, Department of Obstetrics and Gynecology, Nagoya University Graduate School of Medicine, 65 Tsurumai-cho, Showa-ku, Nagoya 466-8550, Japan; t-ume@med.nagoya-u.ac.jp

Accepted 14 July 2010

ABSTRACT
Background Glypican-3 (GPC3), a membrane-bound heparan sulphate proteoglycan, may play a role in promoting cancer cell growth and differentiation. Recent studies reported that GPC3 is overexpressed in clear cell carcinoma (CCC) of the ovary, and not other ovarian histotypes. However, in CCC patients, the relationship between the overexpression of GPC3 and prognosis has not yet been clarified.
Aim To evaluate GPC3 expression by immunohistochemistry in CCC.
Methods and Results In 52 CCC patients, GPC3 expression was observed in 40.4%. In cases of CCC, no correlations were identified between GPC3 expression and clinicopathological factors, such as age, FIGO stage, CA125 values, peritoneal cytology, ascitic fluid volume and mortality rate, except for the residual tumour size. GPC3 expression was associated with poor progression-free survival in stage I CCC patients. The numbers of Ki-67-stained cells in GPC3-positive areas were lower than those in GPC3-negative areas. GPC3 expression may be associated with a low proliferation rate in CCC cells. In the early stage of CCC, GPC3-expressing patients tended to be resistant to taxane-based treatment.
Conclusions Results suggest that the overexpression of GPC3 may be related to the low-level proliferation of tumours; it may be associated with resistance to taxane-based chemotherapy and a poor prognosis in CCC of the ovary.

INTRODUCTION

Epithelial ovarian carcinoma (EOC) is the leading cause of death from gynaecological malignancy. Since ovarian carcinoma frequently remains clinically silent, the majority of patients with this disease have advanced intraperitoneal metastatic disease at diagnosis.[1] In addition, various histological types and degrees of malignancy make it complicated to understand and analyse ovarian carcinoma, and the chemosensitivity and biological nature are different among these histological types.[2] Clear cell carcinoma (CCC) of the ovary was originally termed 'mesonephroma' by Schiller in 1939, as it was thought to originate from mesonephric structures and resemble renal carcinoma.[3] Since 1973, CCC has been recognised in the WHO classification of ovarian tumours as a distinct histological entity, and its clinical behaviour is also distinctly different from that of other epithelial ovarian cancers.[4] Several studies have shown that CCC patients exhibit a poor prognosis.[5-9] In the litera-

ture, the low-level response of CCC to conventional taxane-based chemotherapy is associated with a poor prognosis.[10 11] Several reports have shown that the lower-level proliferation of clear carcinoma cells may contribute to their resistance to chemotherapy.[12 13] However, the mechanism of resistance to chemotherapy in CCC has remained unclear.

Glypicans are a family of heparan sulphate proteoglycans that are linked to the exocytoplasmic surface of the plasma membrane through a glycosylphosphatidylinositol anchor. Six glypicans have been identified in mammals (GPC1-GPC6), and two in *Drosophila*.[14] The physiological function of glypicans is still not well understood. However, it was shown that the glypican-3 (GPC3)-encoding gene is mutated in patients with Simpson-Golabi-Behmel syndrome, an X-linked disorder characterised by prenatal and postnatal overgrowth and a varying range of dysmorphisms. GPC3 regulates cell growth either positively or negatively depending on the cell type. Genetic and functional studies showed that glypicans regulate the signalling activity of various morphogens, including Wnts, hedgehogs, bone morphogenic proteins and fibroblast growth factors.[15-19] Previous studies showed that GPC3 was overexpressed in Wilms' tumour, hepatocellular carcinoma and hepatoblastoma.[20 21] In ovarian carcinoma, GPC3 was overexpressed in yolk sac tumour and CCC, and not in other histotypes of EOC.[22-24] In a previous report, we demonstrated that GPC3 was associated with taxol resistance in CCC.[25] Thus, we hypothesised that GPC3 expression was associated with a poor prognosis in CCC patients. Maeda *et al* reported that GPC3 expression was significantly associated with a poor prognosis in stage III/IV CCC cases. However, the majority of clear cell adenocarcinomas are diagnosed at an early stage, and the relationship between GPC3 expression and the prognosis has remained unclear in early-stage CCC cases.

In the present study, we examined the immunohistochemical expression of GPC3 in CCC tissues to determine whether GPC3 expression is correlated with clinicopathological factors or the prognosis of CCC patients, especially in early-stage disease. We also investigated whether GPC3 was associated with CCC proliferation based on immunohistochemistry.

MATERIALS AND METHODS
Patients and tissue samples
Fifty-two human CCC tissue samples were obtained from patients who had undergone surgical
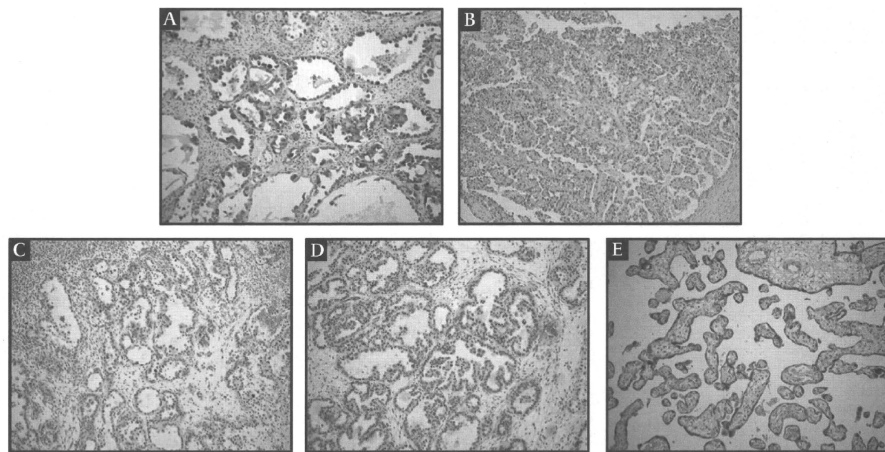
— 94 —

Figure 1 Immunohistochemical staining patterns for glypican-3 (GPC3) in clear cell carcinoma. (A) Strong positive expression of GPC3. (B) Moderate positive expression of GPC3. (C) Weak positive expression of GPC3. (D) Negative expression of GPC3. (E) Positive control for GPC3 (normal placenta).

treatment at Nagoya University Hospital between 1992 and 2006 after giving informed consent. The age of the patients ranged from 27 to 77 years, with a median of 52 years. None of these patients had undergone neoadjuvant chemotherapy before surgery.

All tissue samples were fixed in 10% formalin, embedded in paraffin and routinely stained with H&E for histological examination. All patients received postoperative chemotherapy with platinum plus cyclophosphamide and doxorubicin (before 1997) or platinum plus paclitaxel (after 1997). Tumour recurrence/progression was defined based on the clinical, radiological or histological diagnosis. Chemoresistance was defined as the appearance of a new lesion or a greater than 25% increase in tumour size within 6 months after finishing chemotherapy.

Immunohistochemistry

Formalin-fixed, paraffin-embedded tissue sections were cut at a thickness of 4 μm. For heat-induced epitope retrieval, deparaffinised sections in 0.01 M citrate buffer (Target Retrieval Solution, pH 6.1, Dako, Glostrup, Denmark) were treated three times at 90°C for 5 min using a microwave oven. Immunohistochemical staining was performed using the avidin-biotin immunoperoxidase technique (Histofine SAB-PO kit, Nichirei, Tokyo, Japan). Endogenous peroxidase activity was blocked by incubation with 0.3% hydrogen peroxide in methanol for 15 min, and non-specific immunoglobulin binding was blocked by incubation with 10% normal goat serum for 10 min. The sections were incubated at 4°C for 12 h with primary antibody

against human GPC3 (1:200, clone IG12; BioMosaics, Burlington, Vermont, USA) and Ki-67 (1:200, clone MIB-1, Dako). The sections were rinsed and incubated for 30 min with biotinylated secondary antibody. After washing, the sections were incubated for 30 min with horseradish peroxidase-conjugated streptavidin and finally treated with 3-amino-9-ethyl-carbazole in 0.01% hydrogen peroxide for 10 min. The slides were counterstained with Meyer's haematoxylin. The immunostaining intensity of GPC3 was scored semiquantitatively based on the per cent positivity of stained cells employing a 4-tiered scale as follows: for the evaluation of GPC3 expression,

Table 1 Immunohistochemical staining in clear cell carcinoma patients

Strongly positive	5 (9.6%)
Moderately positive	9 (17.3%)
Weakly positive	7 (13.5%)
Negative	31 (59.6%)

Table 2 Relationship between the expression of glypican-3 (GPC3) and clinicopathological parameters of clear cell carcinoma

		GPC3		
	Number	Negative	Positive	p Value
Total	52	31	21	
Age, years				
≤50	19	13	6	0.33
>50	33	18	15	
FIGO stage				
I	32	17	15	0.22
II—IV	20	14	6	
Residual tumour				
<1 cm	45	24	21	0.02
≥1 cm	7	7	0	
CA125, U/ml				
<250	37	20	17	0.20
≥250	15	11	4	
Peritoneal cytology				
Negative	30	19	11	0.52
Positive	22	12	10	
Ascitic fluid volume, ml				
<100	33	17	16	0.11
≥100	19	14	5	